



Aiola, S. et al. (2021) Hybrid seeding: a standalone track reconstruction algorithm for scintillating fibre tracker at LHCb. *Computer Physics Communications*, 260, 107713. (doi: [10.1016/j.cpc.2020.107713](https://doi.org/10.1016/j.cpc.2020.107713))

This is the author version of the work deposited here under a Creative Commons license: <http://creativecommons.org/licenses/by-nc-nd/4.0/>

Copyright © 2020 Elsevier B.V

There may be differences between this version and the published version. You are advised to consult the published version if you wish to cite from it: <https://doi.org/10.1016/j.cpc.2020.107713>

<https://eprints.gla.ac.uk/307181/>

Deposited on 25 October 2023

Enlighten – Research publications by members of the University of Glasgow
<http://eprints.gla.ac.uk>

Hybrid seeding: A standalone track reconstruction algorithm for scintillating fibre tracker at LHCb

S. Aiola · Y. Amhis · P. Billoir · B. Kishor Jashal · L. Henry* ·
A. Oyanguren Campos · C. Marin Benito · F. Polci · R. Quagliani* ·
M. Schiller · M. Wang

Received: date / Accepted: date

Abstract We describe the **Hybrid seeding**, a standalone pattern recognition algorithm aiming at finding charged particle trajectories for the LHCb upgrade. A significant improvement to the charged particle reconstruction efficiency is accomplished by exploiting the knowledge of the LHCb magnetic field and the position of energy deposits in the scintillating fibre tracker detector. Moreover, we achieve a low fake rate and a small

contribution to the overall timing budget of the LHCb real-time data processing.

Keywords Track reconstruction. pattern recognition. LHCb

Acknowledgements We would like to thank A. Hennequin for many fruitful discussions. We also thank the LHCb RTA team for supporting this publication and reviewing this work. We thank the technical and administrative staff at the LHCb institutes.

R. Quagliani acknowledges support of the European Research Council Consolidator grant RECEPT 724777.

L. Henry and S. Aiola acknowledge support of the European Research Council Consolidator grant SELDOM 771642.

C. Marin Benito acknowledges support of the Agence Nationale de la Recherche grant BACH.

*Corresponding authors: Louis Henry louis.henry@cern.ch, Renato Quagliani renato.quagliani@cern.ch

R. Quagliani · F. Polci · P. Billoir
LPNHE, Sorbonne Université, Paris Diderot Sorbonne Paris Cité, CNRS/IN2P3, Paris, France

Y. Amhis · C. Marin Benito
Université Paris-Saclay, CNRS/IN2P3, IJCLab, Orsay, France

L. Henry
IFIC, Valencia, Spain and Università di Milano, Milano, Italy

A. Oyanguren Campos · B. Kishor Jashal
IFIC, Valencia, Spain

S. Aiola
Università di Milano, Milano, Italy

M. Schiller
University of Glasgow, UK

M. Wang
Center for High Energy Physics, Tsinghua University, Beijing, China

1 Introduction

The LHCb detector [1] is undergoing a major upgrade in preparation of the Run 3 data taking at the LHC, starting in 2021 [2]. The expected delivered instantaneous luminosity is $\mathcal{L} = 2 \times 10^{33} \text{ cm}^2 \text{ s}^{-1}$, corresponding to an average of seven proton-proton interactions per bunch collision.

The entire charged particle reconstruction (tracking) system of the LHCb detector is renewed as part of this upgrade. In particular, the tracker placed downstream of the LHCb dipole magnet is replaced by a scintillating fibre tracker (SciFi) described in detail in Ref. [3]. The SciFi consists of three stations (T1, T2, T3), each composed of four layers of stacked scintillating fibres. The layers within one station are separated from each other by an air-filled gap of 50 mm and they are oriented in a stereo configuration (x - u - v - x). For the sake of mechanical stability, the scintillating fibres in the x -layers are strictly vertical, so that they have a slight tilt with respect to the y axis, which is perpendicular to the beam axis in the usual LHCb coordinate system. The u/v layers are rotated in the $x - y$ plane by the stereo angle, α , equal to $+5^\circ$ and -5° for the u and v layers, respectively.

An algorithm relying solely on the information provided by this tracker, called **Hybrid seeding**, is described in this paper. This algorithm allows an efficient reconstruction of tracks from particles with momenta down to 1.5 GeV/ c . The track segments reconstructed by this algorithm are used as seed for other pattern recognition algorithms in LHCb.

The LHCb upgrade trigger strategy relies on two software stages called HLT1 and HLT2 [4]. The HLT1 stage performs a partial reconstruction of the event in order to select general heavy-flavour physics signatures, such as tracks from displaced vertices, tracks with high transverse momentum or muons carrying large transverse momentum. The HLT2 reconstruction exploits the reduced event rate after the HLT1 selections to perform a full reconstruction of the event, adding offline-quality particle identification information and aiming at reconstructing all the tracks in the event. This reconstruction also benefits from the real-time alignment and calibration procedure developed for the Run 2 data taking [5]. Within this scheme, and in its current version, the **Hybrid seeding** is designed to be executed within HLT2. The current goal is to run the HLT2 stage at a frequency of 1 MHz using around 1000 CPU nodes [4].

2 Motivation

The LHCb detector at the LHC is specialised in the study of heavy hadrons. Physics analyses in LHCb rely mainly on two track types, called “Long” and “Downstream” as defined in Fig. 1. Long tracks are reconstructed using energy deposits (hits) from at least the vertex locator (VELO) [6] and the SciFi sub-detectors, and represent the majority of tracks used in LHCb analyses. Downstream tracks, which are reconstructed using hits in the upstream tracker (UT) and SciFi, typically correspond to the decay products of long-lived hadrons such as K_S^0 mesons and Λ baryons.

The LHCb track reconstruction [7] consists of two main consecutive steps. First, the pattern recognition algorithms create track segments by connecting hits from the sub-detectors: the VELO, the UT and the SciFi. Second, the track fitting provides the track candidates, with a track quality expressed in terms of a χ^2 per degrees of freedom.

The **Hybrid seeding** [8] is a stand-alone algorithm, *i.e.* it does not rely on any input from other algorithms in the tracking sequence. It produces track segments inside of the SciFi, used later by other pattern recognition algorithms. In addition to allowing the reconstruction of Downstream tracks, these segments can be combined with track segments in the VELO to form Long tracks.

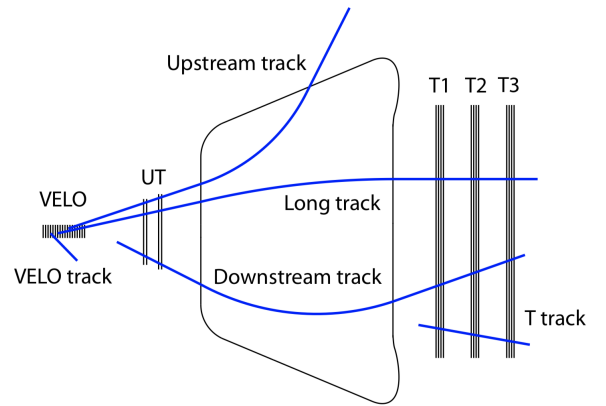


Fig. 1: Track types defined in LHCb. It is worth noting that Long tracks do not need to leave hits in the Upstream Tracker (UT). The SciFi is composed of the T1, T2 and T3 stations, and the LHCb magnet is represented between the UT and the SciFi. Upstream tracks are formed by a combination of hits in the VELO and the UT.

The average occupancy expected in the SciFi in Run 3, shown in Fig. 2, sets a strong challenge for the design of the **Hybrid seeding**: the high hit multiplicity in the central region makes it difficult to identify the correct hits belonging to a given track path. The non-negligible residual magnetic field in the SciFi region further complicates this task, inducing a non-uniform bending of the particle trajectories within the SciFi acceptance. The **Hybrid seeding** has been designed to handle these conditions by exploiting a dedicated parameterisation of the tracks. It provides a high reconstruction efficiency while maintaining a low rate of fake track candidates.

3 The algorithm

The SciFi detector provides measurements of hit positions as (x, z) coordinates, which allow a direct extraction of track patterns in the bending plane of the LHCb detector (along the x direction). The track patterns in the non-bending plane (along the y direction) are measured combining information from the x - z patterns with hits from the u/v layers. For this reason, the algorithm is designed to first build the projection of the track candidates in the x - z plane, called *seed* candidates, by combining measurements from the six x -layers only. Later on, a search for matching hits in the non-bending plane is performed using the information from u/v -layers. The y - z patterns are built through the relation $x_{\text{measured}}^{u/v} - x_z = y_z \times \tan(\alpha)$, where x_z and

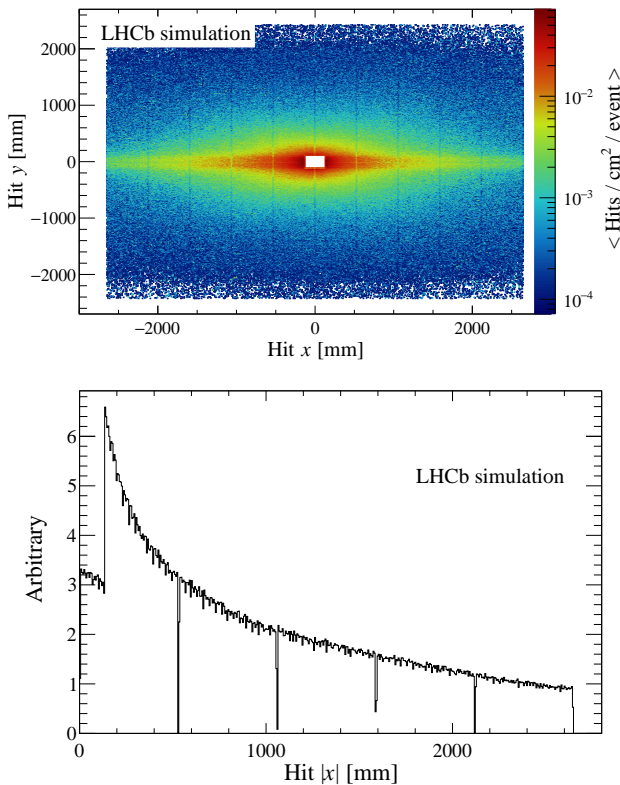


Fig. 2: Top: event average hit density in a single layer of the SciFi. The hole in the middle corresponds to the beam hole. Bottom: information provided after detector readout to the **Hybrid seeding** (y -information is integrated out).

y_z define the true position of a track in the detection layer placed at position z and α is the stereo angle defined in Sec. 1. These two pieces of information can be constrained thanks to a dedicated track model parameterisation. The final output of the **Hybrid seeding** is a 3-dimensional track segment that can be combined with information from other detectors.

The first task of the **Hybrid seeding** is to reduce the number of combinations when finding the hits corresponding to a particle's trajectory. The trajectory of a track with momentum \vec{p} is modelled through a double integration of the equation of motion $d\vec{p}/dt = q\vec{v} \times \vec{B}$, for a particle with charge q and velocity \vec{v} . The residual magnetic field \vec{B} in the SciFi geometrical acceptance can be in first approximation described by $B_x \sim 0$, $B_y = B_0 + B_1 \cdot \bar{z}$, $B_z \sim 0$, where $\bar{z} = z - z_{\text{ref}}$ with $z_{\text{ref}} = 8525$ mm. In the small track angle approximation

$$x(z) = a_x + b_x \bar{z} + c_x \bar{z}^2 (1 + d_x \bar{z}) \quad (1)$$

$$y(z) = a_y + b_y \bar{z}, \quad (2)$$

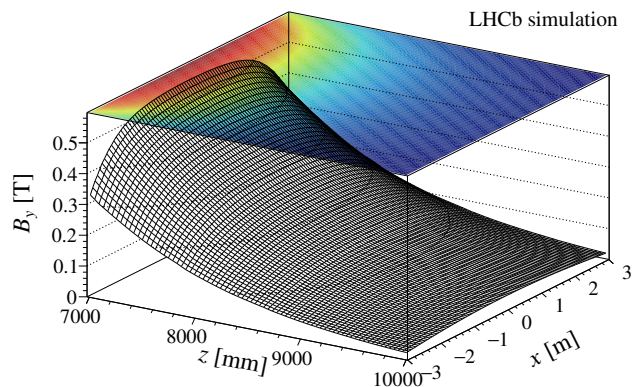


Fig. 3: Dependency of the B_y magnetic field component as a function of the bending plane in the acceptance region of the SciFi detector. The magnetic field intensity decreases as a function of z and can be written in a first approximation as $B_y = B_0 + B_1 \cdot z$, where B_1/B_0 is roughly constant.

where a_x, b_x, a_y, b_y correspond respectively to the usual parameters $x, t_x = dx/dz, y, t_y = dy/dz$ at \bar{z} . The a_x, b_x, c_x, a_y and b_y parameters are left free in the track fit. The d_x parameter, which is equal in this approximation to $B_1/3B_0$, is taken as a constant, estimated from studies on simulated samples. This parameterisation is motivated by the observed variation of the main magnetic field component (B_y) in the LHCb bending plane, as shown in Figure 3.

A path to collect hits is defined using search windows assuming that the tracks originate from $(0, 0, 0)$, which is located inside of the VELO. This hypothesis holds well for all tracks that originate from before the UT. The number of hit combinations to be processed increases with the size of the search window. Therefore, a progressive “cleaning” of the tracking environment is performed in 3 iterations. This allows to open a wide search windows in the last iteration, as needed for the reconstruction of low-momentum particles. This progressive approach is necessary to respect the strict timing constraints of real-time analysis [4] and to keep the rate of fake tracks low. Furthermore, each iteration starts with different pairs of x -layers, one in T1 and one in T3, in order to compensate for hit detection inefficiency, due to either the fibres themselves (1–3% depending on irradiation [3]) or inactive zones between fibre mats. Table 1 gives the layers used in each iteration along with their momentum range. The indices “x1” and “x2” designate the first and second x -layer of a given station, respectively.

For each hit in the first layer, a search window is opened in the second layer, according to the considered

Table 1: Definitions of the iterations in the LHCb implementation. All search windows are tuned according to simulated tracks that satisfy the momentum condition.

Iteration	1	2	3
First x -layer	T1x1	T1x2	T1x1
Second x -layer	T3x2	T3x1	T3x1
Minimum momentum	5 GeV/c	2 GeV/c	1.5 GeV/c

momentum range, expected charge disparity in different halves of the detector due to the magnetic field, and assuming that the tracks originate from $(0,0,0)$, as illustrated in Figure 4. The windows are kept wide enough so that the efficiency is large for all particles created before the magnet and for electrons, which can lose energy due to the bremsstrahlung effect [9]. For each pair of hits, together with the assumption that the track comes from the origin, a momentum hypothesis is derived and used to predict the region in each of the x -layers of the T2 station where a hit from the corresponding track is expected. Once a third hit is found in T2, a curve is defined and remaining hits from leftover x -layers are searched for along it to form a track candidate. Only track candidates with at least five hits, each in a different x -layer, are selected. A fit is then performed according to Eq. 1 and track candidates are filtered using a χ^2 per degree of freedom criterion. In this process, outlier hits can be removed, down to a minimum of four hits.

Hits processed in this phase of the **Hybrid seeding** are sorted by layer and increasing x coordinate. For a given momentum hypothesis and pair of seed layers, the boundaries of the two-hit search windows are monotonously increasing in x . As a result, the search for the second hit is significantly sped up by caching search bounds. This approach is replicated for the search of the third hit, and of remaining hits, as two-hit combinations corresponding to the same first hit are naturally sorted by slope. Finally, the position of the first hit in T2 that matches a two-hit combination built from a given hit in T1 is saved. The next search for the third hit starts from the previously formed two-hit combination. This optimisation allows to move the search window in each T2 layer by only a few hits when iterating over T1 hits.

Only about a third of x - z candidates are real tracks, the rest are fake combinations. Using $x(z)$ from Eq. 1, acceptance windows are defined in the six u/v layers of the SciFi, and hits are collected. It is worth noting that, due to the arrangement of fiber mats in the u/v layers, tracks that belong to the $y > 0$ plane could have hits in the lower part of the layer, and conversely. This

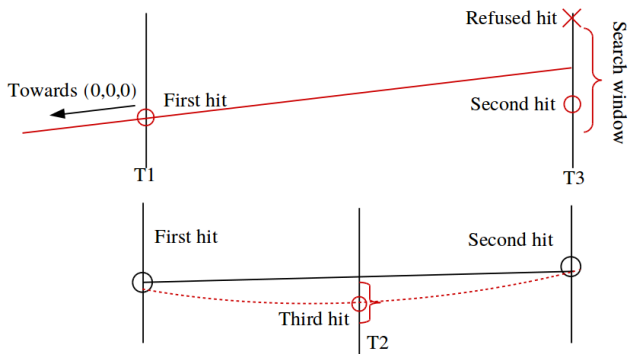


Fig. 4: Illustration of the two- and three-hit searches in the x - z plane.

is accounted for by considering both halves of the detector in the hit collection part. Each of the collected hits, along with the $x(z)$ track equation, corresponds to a possible y measurement, as well as a track slope $t_y(z_0) = y/(z_{\text{layer}} - z_0)$ measurement. In a dipolar magnetic field along the y direction, tracks coming from a given $(0,0,z_0)$ point with low values of t_x and t_y are expected to have a quasi constant $t_y(z_0)$. The current implementation of the **Hybrid seeding** is tuned towards the reconstruction of tracks coming from the interaction region, so it only performs searches for tracks with constant $t_y(z_0) \simeq t_y(0)$. Although the optimisation is driven by Long tracks, Downstream tracks and electrons are also reconstructed, thanks to the size of the search windows.

The search for $t_y(0)$ clusters is performed using a binned implementation of the ‘‘Hough cluster search’’ [10], with one histogram per u/v -layer. Each bin is set to zero if no corresponding $t_y(0)$ value is found, and one otherwise. An additional attribute of the Hough cluster search algorithm stores the address of hits corresponding to filled bins. Once the histograms are filled, looking for an actual cluster amounts to summing the values of the six histograms, bin-per-bin, and looking for a bin with a value four or higher, the actual criterion depending on parameters of the algorithm. When several clusters are found, typically in events with high multiplicity and in busy regions of the detector, only the three largest ones are kept. A fit is performed on each of the retained clusters, and the hits matching the best linear fit are added to the x - z candidate. It should be noted that the y - z fit model does not enforce any constraint on the origin of the track, thus downstream tracks are not rejected by this step. The total candidate track is fitted using the full track model defined in Eq. 1 and filtered using additional χ^2 criteria. Finally, an additional criterion based the track χ^2 and

the number of hits on the segment is applied to tracks in order to determine whether to flag hits belonging to them. Hits that are flagged to belong to high-quality tracks are not considered in further iterations of the search.

After the previous process has been repeated few times, to cover the whole desired momentum range, a recovery routine is employed to recycle x - z projections for which a final track candidate could not be built by adding u/v hits. The recycled x - z projections are required to share no hit with any confirmed candidate, in order to reprocess only x - z projections that are likely to be associated to a new track candidate. When those candidates are recovered, the u/v information is added in the same manner as explained earlier but with enlarged search windows for the track criteria selections.

Finally, a clone removal procedure is applied, checking for closest approach of different tracks in T1/2/3 and the number of shared hits. In the case where two tracks are determined to be clones of each other ($> 70\%$ shared hits on a given track), the one with the largest number of hits is retained and, in case of equality, the one that has the lower χ^2 from the fit using the full track model is retained.

4 Performance

As detailed in Section 2, the aim of the **Hybrid seeding** algorithm is to reconstruct tracks with very different kinematical and topological properties with the highest possible efficiency. Table 2 displays the efficiencies of the **Hybrid seeding** over different types of tracks, as calculated using samples of 1000 simulated events. Tracks are considered as reconstructible in the SciFi (“Has T”) if they leave a hit in at least one layer in each station. In Table 3, the evolution of the fake rate is investigated for various simulated events.

The simulated physics samples are selected to reflect the ambitious LHCb physics program. The efficiency is close to or larger than 90% for all types of tracks that are relevant to LHCb physics analyses, i.e. Long and Downstream tracks. The inefficiency is due to selection criteria and to the hypotheses made in the **Hybrid seeding** algorithm, as described in Sec. 3, which favour tracks from primary interactions or short-lived decays. Furthermore, almost half of the tracks originating from secondary interactions with the detector are reconstructed, which allows to match them with the corresponding energy deposits in the calorimeter in order to tag the calorimeter clusters as “charged”.

Figure 5 shows the dependence of the efficiency on the pseudorapidity and the momentum of the tracks, as

Table 2: Efficiencies (ϵ) for different kinds of tracks, as obtained from simulated samples of 1000 events. The “Has T” requirement states that a given track has at least one associated hit in each T station, and would then be reconstructible by an ideal algorithm. Long-lived is defined as having a segment in the UT and T stations, but not in the VELO. The “h.i.” and “p.p.” labels refer to “hadronic interaction” and “pair production”, respectively, which are the two categories of material interaction creating charged tracks in the detector. If not specified otherwise, the tracks are created through decay of particles originated in a primary vertex.

Sample	Track type	ϵ [%]
$B_s \rightarrow \phi\phi$	Not e^\pm	82.0
$B_s \rightarrow \phi\phi$	Has T	43.3
$B_s \rightarrow \phi\phi$	Has T, from h.i.	
$B_s \rightarrow \phi\phi$	Not e^\pm , $2 < \eta < 5$	
$B_s \rightarrow \phi\phi$	Long	92.4
$B_s \rightarrow \phi\phi$	Long, $p > 5$ GeV/c	95.4
$D^* \rightarrow (D \rightarrow K\pi)\pi$	Long, from D	93.5
$D^* \rightarrow (D \rightarrow K\pi)\pi$	Long, from D, $p > 5$ GeV/c	96.4
$D^+ \rightarrow K_S^0\pi^+$	Long-lived	90.0
$D^+ \rightarrow K_S^0\pi^+$	Long-lived, $p > 5$ GeV/c	95.2
$B_s \rightarrow \phi\phi$	Long, from h.i.	87.4
$B \rightarrow K^{*0}e^+e^-$	e^\pm , $2 < \eta < 5$	
$B \rightarrow K^{*0}e^+e^-$	Long	89.4
$B \rightarrow K^{*0}e^+e^-$	Long, $p > 5$ GeV/c	90.7
$B_s \rightarrow \phi\phi$	Has T, from p.p.	49.6
$B_s \rightarrow \phi\phi$	Long, from p.p.	85.0

Table 3: Fake rate and average fake rate as function of the simulated decay, calculated using 1000 events of each. The fake rate is defined as $\sum_{\text{event}} n_{\text{fake}} / \sum_{\text{event}} n_{\text{reconstructed}}$, while the average fake rate is defined as $1/N_{\text{events}} \cdot \sum_{\text{event}} (n_{\text{fake}}/n_{\text{reconstructed}})$.

Simulated decay	Fake rate [%]	Average [%]
$B \rightarrow K^{*0}e^+e^-$	9.9	6.5
$B_s \rightarrow \phi\phi$	11.7	6.8
$D^{*+} \rightarrow (D^0 \rightarrow K^-\pi^+)\pi^+$	10.7	6.5
$Z \rightarrow \mu^+\mu^-$	14.7	8.1
Minimum bias	7.7	4.9

well as the number of primary vertices. Efficiency saturates at around 95% for non-electron, high-momentum tracks, and decreases slightly with increasing number of primary vertices. This is related to the increasing complexity of the underlying event. Additionally, on Fig. 6 the dependence of the fake rate on the number of primary vertices is shown, demonstrating an increasing trend with more primary vertices, as expected. The larger fake rate at small number of primary vertices can

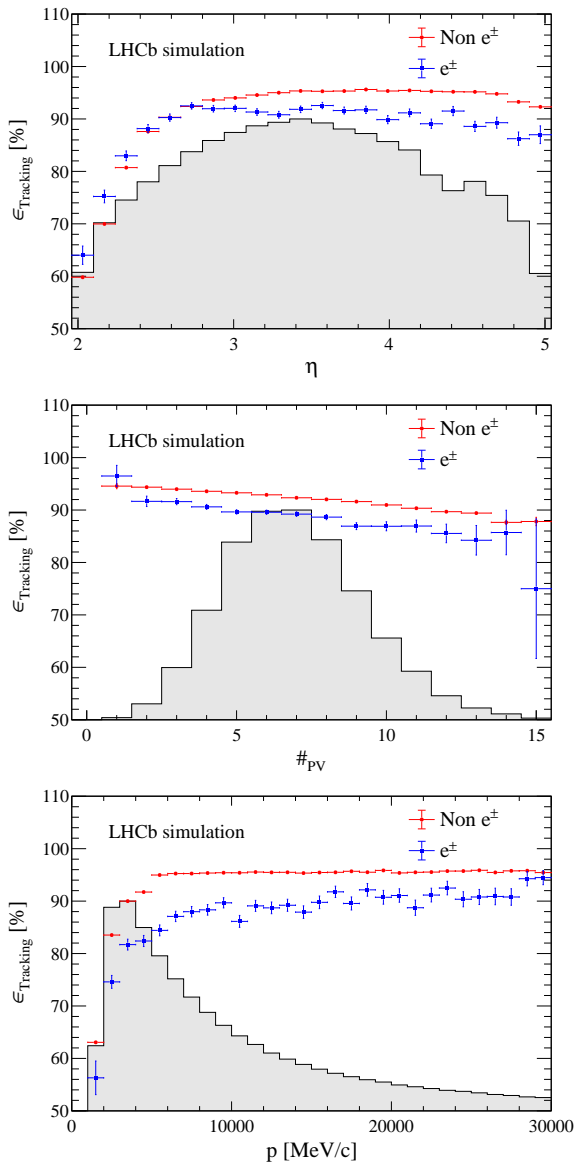


Fig. 5: Dependency of the seeding efficiencies with respect to (top) pseudorapidity, (middle) the number of primary vertices and (bottom) momentum. Blue and red refer to electron and non-electron tracks, respectively. Tracks are taken within the $2 < \eta < 5$ interval.

be attributed to an increased proportion of noise and hits from other bunch-crossings.

Table 4 shows the share of the HLT2 timing dedicated to the **Hybrid seeding** algorithm in September 2019 and June 2020, along with the total throughput of the HLT2 sequence on a reference dual Intel-Xeon-CPU-E5-2630-v4 node. Using a naive extrapolation by dividing the total throughput by the timing share, the estimated throughput of the seeding sequence has then jumped from around 800 Hz/node to around

Table 4: Overall throughput of the HLT2 sequence, as well as the timing share dedicated to the seeding and an estimate of the seeding-only throughput.

	Sept. 2019	June 2020
HLT2 throughput [Hz]	90	122.5
Seeding share [%]	11	3.5
Seeding throughput [Hz]	818	3441

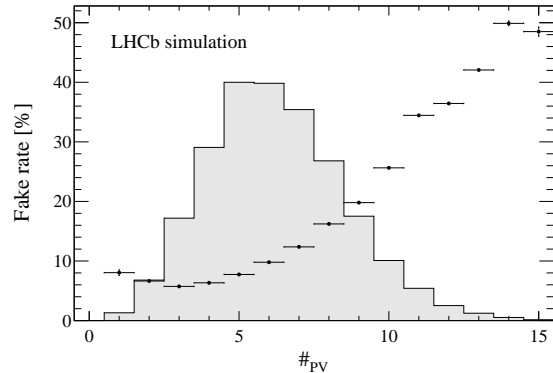


Fig. 6: Dependency of the seeding fake rates as a function of the number of primary vertices in the event.

3.4 kHz/node. This increase in speed has been made possible through many improvements, the most relevant being

- a modernisation of the C++ code;
- a better hit caching and exploitation of the inherent ordering of hit containers;
- the replacement of an unbinned Hough cluster approach by the current binned one, which preserves ordering and layer information;
- the pre-caching of topological information for a fast parabola and tolerance window calculation.

Finally, the timing breakdown and physics performance of the **Hybrid seeding** is comparable to an alternative approach that builds Long tracks starting from VELO segments instead [3]. This ensures that the **Hybrid seeding** can play a complementary role in the reconstruction of Long tracks, which form the core of the LHCb physics program.

5 Conclusion

We have presented an implementation of the **Hybrid seeding**, a pattern recognition algorithm designed to reconstruct track segments using information from the SciFi tracker installed for the LHCb upgrade. The use of an iterative approach allows to handle the high mul-

tiplicity of hits in the detector, while keeping high efficiencies on a variety of tracks and a low fake rate. Performance studies show that this algorithm improves the reconstruction efficiency for a wide range of particles with respect to the former baseline presented in Ref. [3]. It is currently compatible with the timing and efficiency constraints of real-time analysis [11], and therefore belongs to the baseline scenario of the LHCb trigger in Run 3.

References

1. LHCb collaboration, A. A. Alves Jr. *et al.*, *The LHCb detector at the LHC*, JINST **3** (2008) S08005.
2. LHCb collaboration, *Framework TDR for the LHCb Upgrade: Technical Design Report*, CERN-LHCC-2012-007, 2012.
3. LHCb collaboration, *LHCb Tracker Upgrade Technical Design Report*, CERN-LHCC-2014-001, 2014.
4. LHCb collaboration, *LHCb Trigger and Online Upgrade Technical Design Report*, CERN-LHCC-2014-016, 2018.
5. R. Aaij *et al.*, *Performance of the LHCb trigger and full real-time reconstruction in Run 2 of the LHC*, JINST **14** (2019) P04013, [arXiv:1812.10790](#).
6. LHCb collaboration, *LHCb VELO Upgrade Technical Design Report*, CERN-LHCC-2013-021, 2013.
7. LHCb collaboration, R. Aaij *et al.*, *Measurement of the track reconstruction efficiency at LHCb*, JINST **10** (2015) P02007, [arXiv:1408.1251](#).
8. R. Quagliani, *Study of double charm B decays with the LHCb experiment at CERN and track reconstruction for the LHCb upgrade*, 2017. Ph.D. thesis, presented Oct 6th 2017.
9. LHCb collaboration, R. Aaij *et al.*, *Measurement of the electron reconstruction efficiency at LHCb*, JINST **14** (2019) P11023, [arXiv:1909.02957](#).
10. P. V. Hough, *Method and means for recognizing complex patterns*, 1962. US Patent 3,069,654.
11. LHCb collaboration, *LHCb Upgrade GPU High Level Trigger Technical Design Report*, CERN-LHCC-2020-006, 2020.